Modulated surface-plasmon resonance for adsorption studies

C. F. Eagen
Research Staff, Ford Motor Company, Dearborn, Michigan 48121

W. H. Weber
Research Staff, Ford Motor Company, Dearborn, Michigan 48121
and Physics Department, University of Michigan, Ann Arbor, Michigan 48109
(Received 8 December 1978)

Surface-plasmon resonance (SPR) on high-reflectivity metals is very sensitive to changes in the optical properties of the surface region, in particular, to the effects of adsorbed molecules. We excite the SPR on noble-metal films using the Kretschmann configuration and detect the SPR via the surface-roughness-scattered light. By modulating the angle of incidence of the exciting laser beam and using the electronically differentiated signals to track and monitor the resonance, we are able to measure, as a function of time, the complex dielectric constant of the film and the strength of the surface-roughness scattering. We use this technique to study the chemisorption of O_2 on Cu and Ag where we are able to detect the presence of a fractional monolayer of physisorbed O_2 on the Ag film after the chemisorption is essentially complete. Data on the optical constants obtained from the metal-vacuum interface of *in situ* grown Ag, Cu, and Au films are presented. We also present data on the strong physical adsorption of 1,2-dichloroethane on room-temperature Ag films. At elevated temperatures, the dichloroethane attacks and roughens the surface. The increased roughness allows us to establish an upper limit of 1% for the contribution of the roughness scattering to the width of the SPR on the clean Ag film.

I. INTRODUCTION

Optical surface-plasmon resonance (SPR) was first demonstrated by Otto[1] in 1968. The method has been used subsequently in a wide variety of experiments on thin metal films.[2-8] Recently, it was shown that with the increased sensitivity provided by angle-modulation techniques the SPR can be used to study the optical response of adsorbed molecules in the submonolayer regime.[9] In this paper we discuss these angle modulation techniques in more detail than has been done previously, and show how they can be used to study the growth rate of oxide layers, chemisorption, physisorption, and the chemical attack of films by reactive gases. In particular, we present data on the chemisorption of O_2 on *in situ* grown Cu and Ag films, the physisorption of O_2 on Ag films after the chemisorption is essentially complete, and the physisorption of 1,2-dichloroethane on oxygen-exposed Ag films and the subsequent chemical attack which occurs at elevated temperatures. We also present data on the optical constants obtained from the metal-vacuum interface of *in situ* grown Ag, Cu, and Au films.

The SPR is sensitive to small quantities of adsorbed molecules because it is a high-Q resonance. That is, the surface-plasmon wave propagation distance is long compared to its wavelength; this enables it to respond coherently to the small optical perturbation of adsorbed molecules. Because the real part of the surface-plasmon wave vector, $\mathrm{Re}(k_{sp})$, propagating along a metal-dielectric interface is greater than the wave vector of a free photon in the dielectric, the SPR cannot be excited by direct coupling with incident radiation. Otto[1] circumvented this problem by coupling the evanescent tail exhibited in total internal reflection from a prism across a small air gap to excite the SPR on a Ag film. Similarly, one can excite the resonance on the vacuum-metal interface of a thin film grown directly on a prism by coupling through the film.[10] This method of excitation, which is used in our experiments, is often referred to as the Kretschmann configuration and is illustrated in Fig. 1.

There are two methods in use for detecting the SPR. The most common one involves measuring the attenuated total reflection (ATR) as a function of frequency for fixed prism angle or as a function of prism angle at fixed frequency. The other method measures the scattered light (SL) coupled out by the surface roughness of the film and is usually done at fixed frequency as a function of prism angle. The SL detection scheme has certain experimental advantages over ATR.[5] The greatest advantage is that for highly reflecting films the SL signal exhibits a Lorentzian line shape[4] as a function of prism angle. The measured peak position and half-width at half maximum of this line determine directly the real and imaginary parts of k_{sp}. In addition, since the intensity of the detected signal is proportional to the strength of the surface-roughness scattering, it can be used to

detect small changes in the surface roughness.

It is the simplification of a Lorentzian line shape which allows us to employ angle modulation. By modulating the angle of incidence of the exciting light beam and using the electronically differentiated SL signals both to track and monitor the resonance, the time dependence of both the real and imaginary parts of k_{sp}, as well as changes in the strength of the surface-roughness scattering, can be determined. Because angle modulation allows an accurate determination of small changes in the position and width of the resonance, this method is well suited for monitoring small perturbations in optical response caused by adsorbed molecules.

As is the case for other surface optical probes such as ellipsometry and surface-reflectance spectroscopy, the analysis of SPR experiments allows the determination of an effective dielectric constant for known or assumed film thickness. However, SPR is a more restrictive probe than these traditional spectroscopies in that it can be used only in a limited spectral region on high-reflectivity materials. The useful frequency region is limited at high frequencies by either the asymptote of the surface-plasmon dispersion curve, $\omega=\omega_p/\sqrt{2}$, where ω_p is the bulk plasma frequency, or by the onset of interband transitions. If $\epsilon(\omega)$ is the dielectric function of the metal, a necessary condition for the existence of a sharp SPR is that the $-\mathrm{Re}(\epsilon)$ be large compared with the $\mathrm{Im}(\epsilon)$. The low-frequency limit occurs when the surface-plasmon dispersion curve merges with the light line. The limit arises from the experimental condition that one must be able to excite and detect the surface-plasmon waves as well-defined modes over the range of the independent variable used to measure the SPR. Since we scan the parallel component of the incident wave vector at constant frequency and measure the position and width of the Lorentzian SL signal, this condition implies that the separation of the surface-plasmon dispersion curve from the light line must exceed the width of the resonance, i.e.,

$$\mathrm{Re}(k_{sp})-\omega/c>\mathrm{Im}(k_{sp}). \tag{1}$$

With the dispersion relation for a semi-infinite metal bounded by vacuum,

$$k_{sp}=\omega/c[\epsilon/(\epsilon+1)]^{1/2}, \tag{2}$$

and the Drude expression for the dielectric function,

$$\epsilon=1-\omega_p^2[\omega(\omega+i/\tau)]^{-1}, \tag{3}$$

condition (1) reduces to

$$\omega\tau>1 \tag{4}$$

in the limit of $\omega\ll\omega_p$ and $1/\tau\ll\omega_p$. This condition is identical to the condition that the Q of the metal described by Eq. (3) be >1. It is important to realize that the Q of the resonance, $|\mathrm{Re}(k_{sp})/\mathrm{Im}(k_{sp})|$, can still be large even when condition (4) is violated. Thus the effective low-frequency limit is not not necessarily a condition on the ability of the metal to support long-lived surface-plasmon excitations.

II. GENERAL PRINCIPLES

For a discussion of the type and nature of surface-plasmon modes on metals we refer the interested reader to the review articles by Raether,[11] Economou and Ngai,[12] and the reference therein. For our purposes it is sufficient to note that that the SPR can be treated within the framework of the macroscopic Maxwell equations employing a local approximation for the dielectric function. If the parent metal film and subsequent adsorbed layers are treated as isotropic homogeneous layers separated by mathematically sharp boundaries, then the SPR can be described by the standard Fresnel expressions[13,14] for the transmission $t_{1,n}$ and reflection $r_{1,n}$ coefficients which relate the amplitudes of the fields transmitted through and reflected from the n-layer system to the amplitude of the incident field. For a p-polarized incident wave these coefficients can be obtained by repeated application of the series of relations:

$$t_{1,n}=t_{1,n-1}t_{n-1,n}\exp(ik_{n-1}d_{n-1})/D_n, \tag{5}$$

$$r_{1,n}=r_{1,n-1}+t_{1,n-1}t_{n-1,1}r_{n-1,n}\exp(i2k_{n-1}d_{n-1})/D_n, \tag{6}$$

$$D_n=1-r_{n-1,1}r_{n-1,n}\exp(i2k_{n-1}d_{n-1}), \tag{7}$$

$$r_{n,n+1}=\frac{\epsilon_{n+1}k_n-\epsilon_n k_{n+1}}{\epsilon_{n+1}k_n+\epsilon_n k_{n+1}}, \quad t_{n,n+1}=1+r_{n,n+1}, \tag{8}$$

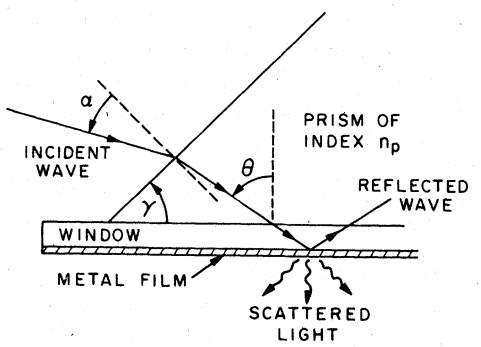

FIG. 1. Geometry for surface-plasmon excitation; $\gamma=44.958$ deg and $n_p=1.514\,34\pm0.0002$.

and

$$k_n = [\epsilon_n(\omega/c)^2 - k_{\parallel}^2]^{1/2}. \quad (9)$$

In these equations ϵ_n is the complex dielectric function of the nth layer and d_{n-1} is the thickness of the $n-1$ layer. The real quantity $k_{\parallel}$ is the component of the wave vector of the incident wave tangent to the film surfaces and is given by $(\omega/c)n_p \sin\theta$, where n_p is the prism index and θ is the angle of incidence at the inside surface of the prism. By Snell's law, $k_{\parallel}$ is identical in each layer. Equations (8) are used first to define the transmission and reflection at a single interface separating two media. These expressions can then be used in Eqs. (5)–(7) to evaluate the fields for the three-layer problem. Successive application of Eqs. (5)–(7) allows one to evaluate the fields for $n > 3$ where the coefficient $r_{n-1,1}$ is evaluated from the known expression for $r_{1,n-1}$ by formally replacing the index 1 by $n-1$, 2 by $n-2, \cdots$, and $n-1$ by 1.

The surface-plasmon modes are defined by examining the conditions necessary for the existence of reflected and transmitted waves in the absence of an incident wave. This implies that both $t_{1,n}$ and $r_{1,n}$ be infinite or, equivalently, that $D_n = 0$. In general, the condition $D_n = 0$ can be satisfied only if $k_{\parallel}$ is allowed to assume complex values. Caution must be exercised in choosing the phases of the k_n [see Eq. (9)] when $k_{\parallel}$ is allowed to be complex. The $\mathrm{Re}(k_1)$ must be positive to insure that the reflected wave propagates away from the surface, and $\mathrm{Im}(k_n)$ for $n \geq 2$ must be positive so that the waves are attenuated in the direction of propagation. To save confusion, we let k_{sp} denote the solutions of the dispersion relation $D_n = 0$ obtained by extending $k_{\parallel}$ into the complex plane. If k_{sp} can be obtained directly from experiment, then the dispersion relation gives a relation between the dielectric constant of a film and its thickness. For example, consider the case of a metal film grown directly on a prism of known refractive index. Since ω and ϵ_1 of the prism, and ϵ_3 of vacuum are known, the condition $D_3 = 0$ defines a relationship between ϵ_2 of the metal, d_2, and k_{sp}. If d_2 is known from separate measurement, then the measurement of k_{sp} determines ϵ_2. Once the optical response of the parent film has been determined, one can proceed to the study of overlayers deposited on the metal film where the measured shifts in k_{sp}, together with the dispersion relation $D_4 = 0$, formally determine an effective dielectric constant ϵ_3 of the overlayer as a function of d_3. In principle this process can be continued as long as one can provide d_3 or ϵ_3 by auxiliary measurement.

We now turn our attention to the experimental determination of k_{sp} and the Lorentzian approximation for the SL line shape. The radiated photons are a result of the scattering of the surface-plasmon waves by inhomogeneities in the dielectric constant of the film. These inhomogeneities can be due to surface roughness, grain boundaries, or other solid-state defects which lie close enough to the film surface to be sensed by the surface-plasmon wave. We make no attempt to distinguish between these sources, and refer to them collectively as the surface roughness. The interaction of the surface wave with the surface roughness excites polarization currents in addition to those induced by the wave on a smooth surface. Treating these currents as a collection of dipole oscillators,[15] one argues that only the component of these currents parallel to the film surface can contribute to the field radiated along the film normal. Since the parallel component of the surface current arises in response to the parallel component of the electric field $E_{\parallel}$ of the surface-plasmon wave, the amplitude of the radiation field will be proportional to $t_{1,n}$.

The transmission function is characterized by a simple pole at k_{sp} and, therefore, can be expressed by its Laurent expansion about this pole. If the pole lies sufficiently close to the real $k_{\parallel}$ axis, $\mathrm{Im}(k_{sp}) \ll 1$, then the amplitude of the SPR can be described adequately by keeping only the first term in this expansion. It is this term which leads directly to the Lorentzian line shape for the SL signal,

$$I(k_{\parallel}) \propto F|S|^2|R|^2/\{[k_{\parallel} - \mathrm{Re}(k_{sp})]^2 + [\mathrm{Im}(k_{sp})]^2\}, \quad (10)$$

where S is the surface-roughness coupling coefficient, F contains such terms as the intensity of the incident light beam and photon detector efficiency, and R is formally the residue of the pole at k_{sp}. Thus the simplification of a Lorentzian line shape allows one to determine k_{sp} by measuring the peak position and width of the resonance as a function of $k_{\parallel}$.

Even when $\mathrm{Im}(k_{sp})$ is small, the SL line shape may not be Lorentzian. This is because the SL method is also sensitive to the scattering of the incident wave by the bulk inhomogeneities of the film and by the surface roughness of the metal-prism interface. The interference of the light scattered from the incident wave with the light scattered from the SPR can lead to serious departures from the Lorentzian line shape.[5] Fortunately, the presence of this parasitic scattered light can be detected by moving off resonance and examining the strength of the background radiation. For our noble-metal films grown on glass substrates at room temperature, the intensity of the signal on resonance is nearly 10^2 larger than the intensity observed far off resonance; thus this

source of error is negligible.

The width of the resonance is sensitive to all processes which attenuate the surface-plasmon wave, including the surface-roughness scattering used to detect the resonance. For extremely rough films, the surface-roughness scattering can broaden the resonance considerably and shift it to higher values of $\mathrm{Re}(k_{sp})$.[16-18] Since the dispersion relation used to infer the dielectric function from k_{sp} does not allow explicitly for this radiation damping, its inclusion results in artificially large values for $\mathrm{Im}(\epsilon)$ of the metal. Therefore if one wants to use the SL method to obtain optical constants for the films that are characteristic of the intrinsic response of the film, it is imperative that the surface-roughness scattering be small. Mills[19] has examined this problem in some detail and shows that in the limit of $|\epsilon| \gg 1$ the attenuation length l due to surface roughness scattering is given by

$$l = \tfrac{3}{4}(c/\omega)^5 |\epsilon|^{1/2}/(a\delta)^2 , \tag{11}$$

where δ is the rms height of the roughness and a is the transverse correlation length. Using in Eq. (11) values of $\delta = 10$ Å and $a = 10^3$ Å typical of Ag films,[20-23] and comparing the calculated attenuation lengths to those obtained experimentally for our films, $[2\,\mathrm{Im}(k_{sp})]^{-1}$, we conclude that across the visible spectrum the attenuation due to roughness scattering is nearly two orders of magnitude smaller than the attenuation due to the intrinsic losses in the metal.

In spite of the above limitations, it is important to realize just how good a Lorentzian approximation for the resonance line shape can be. As a check on both the mathematical approximation and the assumption that the radiated signal is proportional to $|E_{\parallel}|^2$ as obtained from the Fresnel relations, we used the measured width and position of the resonance curve obtained from a 760-Å Ag film at 6328 Å to compute the Ag ϵ from the condition $D_3 = 0$. We then used this ϵ to compute the Fresnel expression for $|E_{\parallel}|^2$ and compared this with the experimental resonance curve. The peak position and half-width of the calculated $|E_{\parallel}|^2$ curve agreed with those of the original resonance curve within our experimental uncertainty. Even the small asymmetry in the wings of the resonance was reproduced faithfully.

In practice we measure the SPR as a function of α, the external angle of incidence on the prism entrance face, which is related to θ by $\sin\alpha = n_p \sin(\theta - \gamma)$, Fig. 1. For small values of α, one has the defining relations

$$\mathrm{Re}(k_{sp}) = (\alpha_m \cos\gamma + n_p \sin\gamma)\omega/c \tag{12}$$

and

$$\mathrm{Im}(k_{sp}) = (\Delta\alpha \cos\gamma)\omega/c, \tag{13}$$

where $\Delta\alpha$ is the half-width of the resonance, α_m the position of the resonance peak, and γ the interior angle of the prism. The choice of a prism angle γ which puts the SPR near normal incidence provides a convenient reference for measuring α and allows one to position the prism and film in the beam in such a way that the beam does not move across the film as α is varied. This is crucial because the diameter of the optic cable, placed ≈ 12 cm away from the film that is used to detect the SPR, is comparable to the size of the illuminated region, and any movement of this region across the film face would change the detection efficiency and distort the shape of the measured resonance. Prescriptions for the prism placement are given in Ref. 5.

We now turn to a discussion of angle modulation and the determination of the time dependence of k_{sp}. If the angle of incidence of the exciting light beam is modulated sinusoidally,

$$\alpha = \alpha_0 + A \sin(\omega_\alpha t), \tag{14}$$

then the detected SL signal at frequency ω_α in phase with the driving signal will pass through zero when $\alpha_0 = \alpha_m$. This signal is used to drive a rotary table, to which the prism and film are affixed, in such a way as to preserve the null in the detected signal. By monitoring the motion of the rotary table, the temporal dependence of α_m can be determined within the limits set by the response time of the servosystem. The width of the SPR and changes in the strength of the surface-roughness scattering are obtained by analyzing the harmonic structure in the SL signal when $\alpha_0 = \alpha_m$,

$$I(t) = F|S|^2/\{[A \sin(\omega_\alpha t)]^2 + (\Delta\alpha)^2\}. \tag{15}$$

Although the harmonic structure can be obtained when $A/\Delta\alpha \ll 1$ by expanding the denominator, the usual restriction of a small modulation amplitude is not necessary when dealing with a known line shape because the Fourier integral

$$I_n = \frac{2\omega_\alpha}{\pi} \int_0^{\pi/\omega_\alpha} I(t) \cos(n\omega_\alpha t) dt \tag{16}$$

can be evaluated easily. Performing the integrations for $n = 0$ and $n = 2$ with the assumption that the time dependence of F, $|S|^2$, and $\Delta\alpha$ is sufficiently slow compared to the oscillation period that they can be treated as constants, one obtains the relations

$$[\Delta\alpha(t)]^2 = [\Delta\alpha(0)]^2 \frac{I_0(t)}{I_0(0)} \frac{I_2(0)}{I_2(t)} \frac{f(0)g(t)}{f(t)g(0)} , \tag{17}$$

$$\frac{|s(t)|^2}{|s(0)|^2}=\frac{F(0)}{F(t)}\left[\frac{I_0(t)}{I_0(0)}\right]^2\frac{I_2(0)}{I_2(t)}\left[\frac{f(0)}{f(t)}\right]^2\frac{g(t)}{g(0)}\ , \qquad (18)$$

where

$$f=[1+(A/\Delta\alpha)^2]^{-1} \qquad (19)$$

and

$$g=f[1+\tfrac{1}{2}(A/\Delta\alpha)^2+f^{-1}]^{-1}\ . \qquad (20)$$

Equations (17) and (18) must be evaluated by iteration starting from the known value of $\Delta\alpha$ at time $t=0$ to evaluate f and g. Notice that F does not appear in Eq. (17) so that fluctuations in the incident light intensity or in the photomultiplier gain do not affect our ability to determine $\mathrm{Im}(k_{sp}(t))$. They do contribute to the surface-roughness signal, Eq. (18). Thus, one must monitor the intensity of the light source and use a very stable photomultiplier when measuring changes in the surface roughness.

III. EXPERIMENTAL

The experiments were done on films grown in a stainless-steel sample chamber equipped with five $2\frac{3}{4}$-in. copper-gasketed flange access ports as shown schematically in Fig. 2. Two optical windows were placed on opposite ports. The film was grown directly on one window and a 6-mm-diam optical cable was used to view the resonance through the other. One side port contains the current leads for the vaporization filament, and the vertical port is connected to a liquid-nitrogen cold trap by flexible metal bellows. This trap in turn is connected to an oil-diffusion pumping station equipped with a second liquid-nitrogen trap. A glass bulb with greased stopcocks is used to expose the film to a known quantity of gas. The chamber was baked at 250°C and the bellows and glass trap at ≈150°C for eight hours before each new film was grown. The glass trap was cooled and filled while the chamber was still hot in order to trap possible contaminants emanating from the O-ring and stopcock located on the pump side of the trap. Final pressures measured at the pump were typically $3-4\times10^{-8}$ torr.

The films were grown by evaporation from a circular tungsten filament positioned concentric with a line joining the center of the two windows. A small annular disk was placed between the filament and the viewing window to prevent any metal deposition on this window while still allowing an unobstructed view of the SPR. Typical film growth rates were from 20–50 Å/sec and final film thicknesses were 700–900 Å. These were monitored during growth by recording the optical transmission of the film. Due to the interference effects

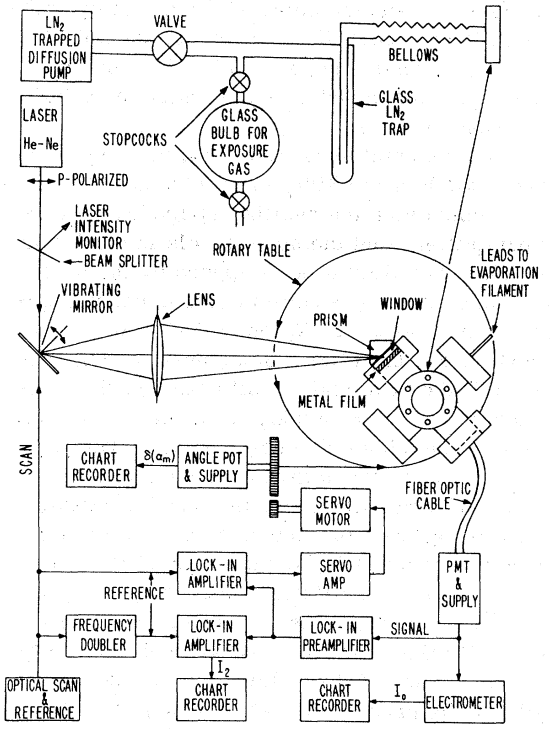

FIG. 2. Schematic drawing of electronic, optical, and vacuum systems employed in angle-modulated SPR studies.

associated with the chamber window, we put the uncertainty at ±10% for the film thickness calculated from the transmission.

The crown glass prism is coupled to the chamber window by means of an index-matching oil, and a small piece of black glass is coupled to the prism exit face to eliminate internal reflections. Studies of SPR intensity versus α are made by reflecting the chopped light beam from a stationary mirror onto the prism and film. The chamber is mounted on a motor-driven rotary table, and the phase detected signal at the chopping frequency is displayed on a chart recorder as a function of the potentiometer voltage which monitors the angular position of the table. Since α is small, the angles are referenced conveniently by reflecting the beam back on itself.

The modulation studies were all done using a He-Ne laser. Here the unchopped beam is reflected from a mirror vibrating at 400 Hz and passed through a lens onto the prism. The purpose of the lens is to keep the beam position fixed on the prism as the angle of incidence is modulated. Angular modulation amplitudes less than the full-width of the resonance, about 0.1–0.2 deg peak to peak, were employed. The SPR signal from the photomultiplier tube is split between the lock-in

amplifiers and electrometer with precautions taken to minimize the capacitive loading of the signal. Ultimately, signals proportional to the shift in α_m, I_0, and I_2 are displayed on strip-chart recorders as functions of time.

The experimental sensitivity is limited by the inherent width of the SPR, the backlash in the table gears coupled with the oscillatory feedback of the servoamplifier, and the noise levels in the I_0 and I_2 signals. The limitations imposed by the SPR width can be seen by examining the harmonic signal I_1 when $\alpha_0 - \alpha_m = \beta$. When $(\beta + A) \ll \Delta\alpha$, I_1 is proportional to $\beta A/(\Delta\alpha)^4$. Since noise considerations limit the practical amplification of this signal, increases in $\Delta\alpha$ quickly limit the deviations β to which the table drive can respond. The backlash in the gears would give an uncertainty in α_m of 0.0015 deg. However, this can be improved by monitoring the table drive, as opposed to its response, and adjusting the damping of the servosystem so that is oscillates within the gear deadspace without appreciable overshoot. By averaging these oscillations visually, we were able to measure shifts in α_m of the order of 5×10^{-4} deg on a Ag film. The precision to which changes in $\Delta\alpha$ can be measured is determined by the uncertainties in both I_0 and I_2, which for a time constant of 0.1 sec are about 1%. However, if one assumes that S is constant, then $[\Delta\alpha(t)/\Delta\alpha(0)]^4 = I_2(0)/I_2(t)$ when $A/\Delta\alpha \ll 1$, and the 1% uncertainty in I_2 legislates a 0.25% sensitivity to changes in $\Delta\alpha$. How these experimental sensitivity limits translate into detectability limits for adsorbed molecules depends on the complex susceptibility of the molecule in its adsorbed state and the width of the parent SPR.

IV. OPTICAL CONSTANTS

Recently, the SPR technique was employed to measure the optical constants of Ag, Au, and Cu films grown on fused-silica substrates.[5] In that study the SPR was excited on the metal-substrate interface by coupling the metal film to a high-index prism using an index-matching fluid. Alternatively, the resonance on the metal-air interface was excited by coupling the substrate to a prism. Their measurements on the metal-air interface consistently yielded values for $|\mathrm{Re}(\epsilon)|$ less than those obtained for the metal-substrate interface. This can be explained by assuming either that the free surface is contaminated by exposure to the air or that the structure of the metal-substrate and metal-air surfaces is different. Therefore, in order to see how closely the optical constants obtained from a metal-vacuum interface can agree with those obtained from the metal-substrate interface when the problems of surface contamination have been minimized, we measured the optical constants of our *in situ* grown Ag, Au, and Cu films. Measurements were made at the wavelengths provided by the He-Ne laser and the filtered lines of a Hg lamp. In order to correct for the experimental broadening of the SPR introduced by the angular spread in the beam of the Hg lamp, the experimental configuration was modified to provide an incident beam of known, controllable angular divergence. Measurements were then made at several values of the beam divergence, and the results were extrapolated to obtain a value for $\Delta\alpha$ corresponding to a perfectly collimated beam.

After growth, all of the films exhibited substantial room-temperature annealing as evidenced by a narrowing of the SPR peak and a shift of the peak towards the light line. These effects are most pronounced on Cu films, but are clearly observable on both Ag and Au films, as has been noted[24] previously. The magnitude of this effect for a Cu film is shown in Fig. 3, and the time dependence of the optical constants derived from the condition $D_3 = 0$ is shown in Fig. 4. Because of this annealing, our reported optical constants were taken on films at least a day after growth. During this time, the progress of the annealing was monitored to check for possible contamination. Since a contaminant would cause the SPR to broaden and shift away from the light line, any growth of a thick contaminant film, such as an oxide or sulphide, would cause the optical constants to exhibit extrema as a function of time. No such extrema were observed; in fact, the optical constants of the films did not appear to degrade for days after growth. Of course, a saturated film in the monolayer regime could form shortly after growth, and this would be undetectable through annealing stud-

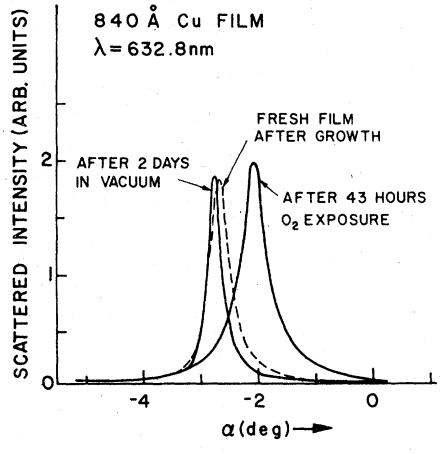

FIG. 3. Experimental dependence of Cu Lorentzian line shape on room-temperature annealing and oxide formation. Each peak is in arbitrary units so that only the peak positions and widths have physical significance.

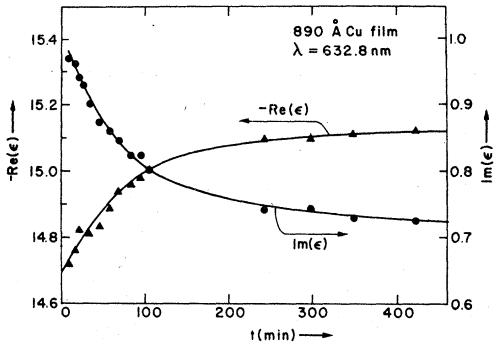

FIG. 4. Effect of room-temperature annealing on the optical constants of a Cu film as measured from the time of growth.

ies. Except for the possibility of a chemisorbed layer exhibiting a strong optical transition, the optical perturbations for monolayer coverages are too weak to alter seriously the measured optical constants of the parent film. Additionally, the rapid reaction with O_2 exhibited by both our Cu and Ag films days after growth argues against the existence of any passivating contaminant.

The results of our measurements are shown in Table I and are compared to the metal-substrate values of Ref. 5. The quoted experimental uncertainties were obtained by computing the deviations in ϵ when the peak position, SPR width, and film thickness were varied independently, and then taking the square root of the sum of the squares of these deviations. Typical uncertainties for position and width were of the order of 0.01–0.02 deg, and a full 10% uncertainty was allowed for the film thickness, which explains the larger uncertainty in Im(ϵ) quoted for our values. These quoted uncertainties only reflect our ability to measure the optical constants of a given film and do not reflect the variations in the values obtained on different films. For example, three Ag films of nominal thickness 750 Å all grown at a rate of ≈ 50 Å/sec yielded values for ϵ at 6328 Å of $-19.56 + 0.709i$, $-19.59 + 0.651i$, and $-19.96 + 0.658i$. Thus it appears that sample-to-sample variation is the limiting factor in determining the uncertainties in the optical constants. Within this limitation our data suggest that there are no systematic differences between the optical constants at the two surfaces of the film.

TABLE I. Comparison of the optical constants obtained for the vacuum interface of Ag, Au, and Cu films, this work, to the values obtained from the metal-substrate interface, Ref. 5.

	λ (Å)	Metal-vacuum interface	Metal-substrate interface
Ag	6907	-24.32 (±0.29) $+0.896i$ (±0.163)	-23.40 (±0.28) $+0.864i$ (±0.066)
	6328	-19.56 (±0.16) $+0.709i$ (±0.099)	-19.02 (±0.18) $+0.642i$ (±0.049)
	5770	-15.46 (±0.09) $+0.682i$ (±0.078)	-15.17 (±0.10) $+0.541i$ (±0.039)
	5461	-13.28 (±0.05) $+0.543i$ (±0.066)	-13.14 (±0.073) $+0.446i$ (±0.031)
	4358	-6.542 (±0.013) $+0.321i$ (±0.049)	
	4047	-4.893 (±0.013) $+0.302i$ (±0.042)	
Au	6328	-13.204 (±0.062) $+1.146i$ (±0.068)	-13.34 (±0.075) $+0.960i$ (±0.055)
	5770	-8.759 (±0.019) $+1.373i$ (±0.065)	
Cu	6328	-15.06 (±0.090) $+0.850i$ (±0.065)	-15.12 (±0.10) $+0.725i$ (±0.040)

V. ADSORPTION

A. Submonolayer coverages

We now proceed with a discussion of the nature of the response of the SPR to films adsorbed on the metal surface. As mentioned in Sec. II, the measured shifts in k_{sp}, coupled with the dispersion relation $D_4 = 0$, determine formally the dielectric function of the overlayer as a function of its thickness. For thick overlayers, the dielectric function and the film thickness are well-defined quantities, and armed with the knowledge of either, the other can be determined. For chemically or physically adsorbed overlayers of submonolayer coverage, the condition $D_4 = 0$ still allows us to assign coupled numerical values to ϵ_3 and d_3; however, the physical meaning of these macroscopic parameters is uncertain. This uncertainty arises for a variety of reasons. If the adsorbed layer is inhomogeneous, the optical response of an adsorbed molecule will depend strongly on its local environment and a homogeneous dielectric function can at best only represent an unspecified average response. Even if the adsorbed layer is homogeneous, the optical response of each adsorbed molecule will depend upon the optical interactions (Lorentz-Lorenz corrections) between it and the other adsorbed molecules, leading to an anisotropic response function. Further, the SPR is sensitive to any changes in optical response in the first few layers of the metal induced by the bonding with the adsorbate layer. It is difficult to envision how this latter effect might be incorporated conveniently into the framework of an isotropic homogenous film delineated by mathematically sharp boundaries such as is mandated by the Fresnel relations. For a further discussion of the problems in defining effective film parameters, we refer the reader to the literature.[25-30]

In spite of the problems of defining and interpreting film parameters, the measured response of

the SPR to adsorbates of submonolayer coverage can yield valuable qualitative information concerning the adsorption process and quantitative information in the limit of a dilute physically adsorbed overlayer. We now examine the SPR response by using the Fresnel relations and by using perturbation theory applied to the scalar equation governing the propagation of a TM mode in a waveguide.

Let us consider the condition $D_4=0$ in detail. Since the metal film is rather thick, nothing is lost pedagogically and little numerically by considering the simpler problem of a thin overlayer adsorbed on a semi-infinite metal. In the limit of large d_2, the condition $D_4=0$ becomes

$$(\epsilon_3 k_2+\epsilon_2 k_3)(\epsilon_4 k_3+\epsilon_3 k_4)+(\epsilon_3 k_2-\epsilon_2 k_3)\times(\epsilon_4 k_3-\epsilon_3 k_4)\exp(2ik_3 d_3)=0, \tag{21}$$

where ϵ_2, ϵ_3, and ϵ_4 are, respectively, the dielectric constants of the metal, adsorbed layer, and vacuum. The solution of Eq. (21) for k_{sp} in the absence of an adsorbed layer, $\epsilon_3=\epsilon_4$, is given by Eq. (2). Treating the adsorbed layer as a weak optical perturbation so that $|k_3|d_3\ll 1$ and the shift in k_{sp}, δk_{sp}, is small, Eq. (21) can be expanded to yield

$$\delta k_{sp}\sim k_{sp}[ik_2k_4/(\epsilon_2 k_2+k_4)](\epsilon_3-\epsilon_2)(\epsilon_3-1)d_3/\epsilon_3, \tag{22}$$

where we have set $\epsilon_4=1$. For a high-Q resonance, the imaginary parts of k_2 and k_4 are large compared to their real parts, and since ϵ_2 is primarily negative real, the quantity in brackets is essentially a positive real number. Thus we see that a transparent overlayer will change only $\mathrm{Re}(k_{sp})$, while a lossy one will change both $\mathrm{Re}(k_{sp})$ and $\mathrm{Im}(k_{sp})$. We note in passing that since Eq. (22) is quadratic in ϵ_3, a measured shift in k_{sp} can be satisfied by a pair of values for ϵ_3 at fixed d_3. One solution corresponds to placing a layer of molecules next to the metal surface, and the other to degrading the optical response of the metal within a distance d_3 of its surface by lowering slightly the magnitude of $\mathrm{Re}(\epsilon_2)$. Therefore care must be exercised in the numerical solution of $D_4=0$ to insure that one has obtained the solution of the desired conceptual form.

For a dilute homogeneous adsorbate where the Lorentz-Lorenz corrections to the local field are negligible, it seems plausible to assume that

$$\epsilon_3=1+4\pi\chi n_a/d_3\ . \tag{23}$$

In this "dilute-gas" model, χ is the microscopic susceptibility of the adatom in the adsorbed state and n_a/d_3 is the number density, where n_a is the number of adatoms/cm^2, and d_3 is a measure of the distance over which χ is appreciable. Substituting Eq. (23) into Eq. (22), with the restriction that the second term in Eq. (23) be small, we find that to lowest order in n_a,

$$\delta k_{sp}\sim k_{sp}[ik_2k_4/(\epsilon_2 k_2+k_4)](1-\epsilon_2)4\pi\chi n_a\ . \tag{24}$$

Thus, in the dilute limit, the measured values of k_{sp} determine the χn_a product. For a physically adsorbed molecule, the perturbations in the optical response of the molecule and metal caused by the bonding process should be small, and the use of values for χ as determined for the molecule in the gas or liquid phase should yield reliable values for n_a. In contrast, the alterations in the optical response of the molecule and metal caused by a chemical bond can be significant, especially if an allowed electronic transition exists in the energy neighborhood of the SPR, and Eq. (24) cannot be used to provide estimates of coverage using gas phase polarizabilities. In fact, the whole model of confining the changes in optical response associated with chemisorption to a film of thickness d_3 adjacent to an unperturbed metal surface may be unphysical.

Some of the difficulties associated with the mathematically sharp boundaries inherent in the Fresnel treatment can be alleviated by examining directly the wave equation governing the propagation of a surface-plasmon wave on a semi-infinite metal. It has been shown[31] that this equation can be put in self-adjoint form when the homogeneous dielectric function $\epsilon(z)$ is real. The z coordinate is perpendicular to the surface. If the wave equation can be solved for a particular specification of $\epsilon(z)$, standard perturbation theory can be employed to compute the shifts in k_{sp}^2 when $\epsilon(z)$ is replaced by $\epsilon(z)+\delta\epsilon(z)$. The formal expression for the shift is

$$\delta(k_{sp}^2)=\left(k_{sp}^2\int_{-\infty}^{+\infty}dz\,|H_y|^2\frac{\delta\epsilon(z)}{\epsilon(z)^2}+\int_{-\infty}^{+\infty}dz\left|\frac{\partial H_y}{\partial z}\right|^2\frac{\delta\epsilon(z)}{\epsilon(z)^2}\right)\Big/\int_{-\infty}^{+\infty}\frac{dz\,|H_y|^2}{\epsilon(z)}\ , \tag{25}$$

where H_y is the magnetic field. Although $\epsilon(z)$ is restricted to real values, $\delta\epsilon(z)$ is not. To the extent that the adsorption process can be represented by a homogeneous $\delta\epsilon(z)$, Eq. (25) can be used to compute the shifts in the SPR within the limits imposed by the requirement that the effective perturbing potential be small. One obtains the Fresnel results by setting $\epsilon(z)=\epsilon_2$ for $z<0$, $\epsilon(z)=1$ for $z>0$, $\delta\epsilon(z)=\Delta$ for $0<z\,d_3$, and $\delta\epsilon(z)=0$ elsewhere. Evaluation of Eq. (25) shows that $\delta(k_{sp}^2)$ is proportional to $[1-\exp(2ik_3d_3)]$, and in the

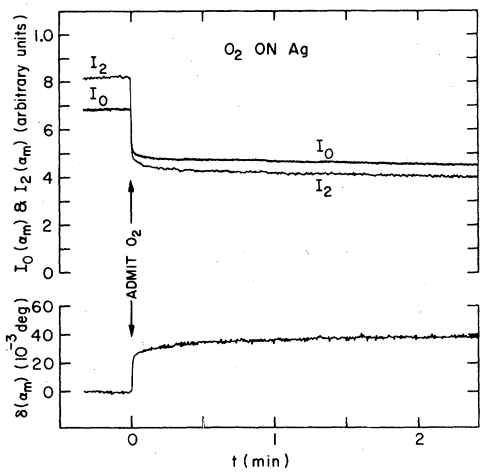

FIG. 5. Response of angle-modulated SPR signals to a 1-torr exposure of O_2 on a clean Ag surface.

limit of $|k_3|d_3 \ll 1$ Eq. (24) is obtained if we identify Δ with $4\pi\chi n_a/d_3$.

We emphasize that Eqs. (22) and (24) have been introduced for pedagogical purposes and are not used to give numerical results. Even for a physically adsorbed molecule, the mathematical restriction of being dilute is quite severe. For example, comparing the values of $\mathrm{Re}(\delta k_{sp})$ computed by means of Eq. (24) and by solving $D_4 = 0$ for physically adsorbed O_2 on Ag, $4\pi\chi = 2.22\times10^{-23}$ cm^3 and $d_3 = 4$ Å, one finds agreement for coverages of less than 0.2 monolayers, but above this

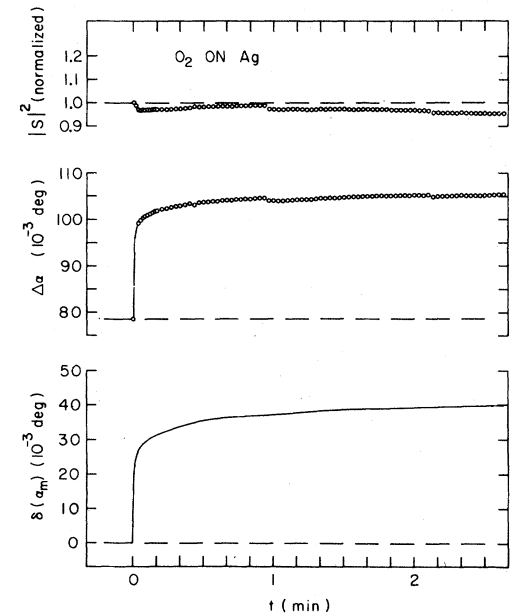

FIG. 6. Change in the resonance width $\Delta\alpha$ and surface-roughness scattering $|S|^2$ from the data in Fig. 5 calculated by means of Eqs. (17)–(20), and a smoothed trace of the change in peak position $\delta(\alpha_m)$.

coverage the values computed from $D_4 = 0$ are less than those obtained from Eq. (24) and differ by roughly a factor of 2 at monolayer coverage. A monolayer is formally defined as one O_2 molecule per Ag atom on a (111) surface.

B. Oxygen

Due in part to the ability of oxygen-exposed Ag surfaces to catalyze the selective oxidation of many organic molecules, the reaction of O_2 with Ag films,[24,32-34] powders,[35,36] polycrystals,[37] and oriented single crystals[38-40] has received much attention in the literature. Although many of the studies are at variance, some of the more recent work suggests that at room temperature O_2 can both adsorb in the molecular state and dissociate to adsorb in the atomic state.[41] The reactivity of O_2 with Ag depends strongly on the cleanliness of the surface and can be modified by the preadsorption of various gases.[33,36] Since our studies do not incorporate a chemically specific spectroscopy, such as Auger electron spectroscopy, which could establish the cleanliness of the Ag surface and the purity of the oxygen layer, the degree to which our results represent the reaction of pure O_2 with clean Ag is moot. However, all the results presented were found to reproduce on films prepared and exposed in identical fashion.

The response of the modulated signals to a 1-torr exposure of O_2 on Ag is shown in Fig. 5. At time $t = 0$ the gas in the bulb is released into the chamber through the liquid-nitrogen cold trap. We calculated exposure pressures using the known volume ratio of the bulb to the chamber. Starting from the measured position α_m and width $\Delta\alpha$ of the SPR before exposure the values of I_0 and I_2 in Fig. 5 at time t determine the width $\Delta\alpha$ and $|S|^2$ at time t via Eqs. (17)–(20) (Fig. 6). Since the absolute value of $|S|^2$ is not determined, it has been set arbitrarily to 1 at $t = 0$. As can be seen from the $\delta(\alpha_m)$ signal, most of the sorption occurs within the first second or two. The adsorption rate then slows markedly, with only about a 1% increase observed in $\delta(\alpha_m)$ between $t = 3$ and $t = 12$ min. The correspondingly rapid increase in $\Delta\alpha$ indicates that the initial adsorption attenuates the 2-eV surface-plasmon wave. The tendency of the $\Delta\alpha$ curve to mimic the $\delta(\alpha_m)$ curve suggests that the O_2 adsorbed after 2 sec has an optical response not dramatically different from that adsorbed during the rapid sorption. The invariance of $|S|^2$ indicates that the adsorbate tends to preserve the surface topography of the parent Ag film.

After the growth had saturated effectively, the residual gas was removed. Pumping on the film for 30 min only reduced $\delta(\alpha_m)$ by a few percent at most, indicating that very little of the adsorbate

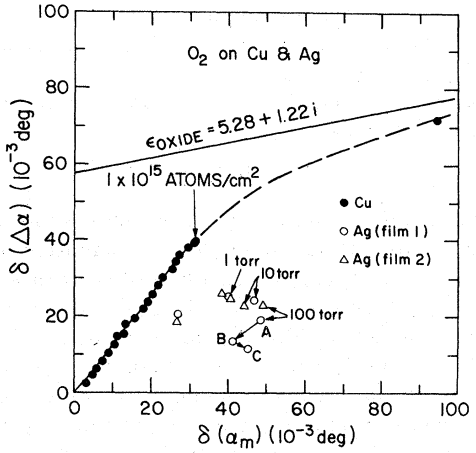

FIG. 7. Compilation of the SPR response for various O_2 exposures on Cu and Ag. A plot showing the growth of a Cu-oxide layer at higher values of $\delta(\alpha_m)$ and $\delta(\Delta\alpha)$ is given in Ref. 9. The straight line is the extrapolation of the linear dependence associated with the oxide growth back into the region of low coverage.

can be removed by pumping for short times. Subsequent exposures at 1 torr produced no further shifts in $\delta(\alpha_m)$ or in $\Delta\alpha$. When the exposure pressure was increased to 10 torr, $\delta(\alpha_m)$ exhibited a substantial increase, tending to saturate after 30 sec with half of the shift occurring in the first 3 sec. Surprisingly, $\Delta\alpha$ did not increase during the 10-torr exposure; in fact, it tended to decrease, indicating that the surface plasmon is attenuated less on a film exposed at 10 torr than on one exposed at 1 torr. The fact that the shift in $\delta(\alpha_m)$ for 30 sec at 10 torr is substantially greater than the shift observed for the preceding 5 min at 1 torr indicates that the adsorption is pressure driven. This observation is consistent with the data of Czanderna[35] on reduced Ag powders, which show the mass uptake after 200-min exposures at 11, 1.1, and 4×10^{-3} to bear the ratios 100: 65: 50, respectively. Again, little adsorbate is removed by pumping for short times, and little is added by further exposure at 10 torr. At 100 torr the surface is again active, with the shifts occurring over the first minute after exposure.

This behavior is summarized in Fig. 7, where we have plotted $\delta(\Delta\alpha)$ against $\delta(\alpha_m)$ for various exposures. The datum point below 1 torr for film 1 was obtained from the adsorption curve 2 sec after exposure, Fig. 6. The two points for film 2 are the result of a planned exposure at 1 torr when the valve to the pump was inadvertently left open and a point from the adsorption curve taken on the subsequent 1-torr exposure. The shift of point A to B was obtained by pumping on the film overnight. The shift from B to C is the result of a subsequent 100-torr exposure for 20 min. Although it is clear that the surface must change during the overnight pumping by either desorbing O_2, absorbing O into the bulk, or rearranging to expose active sites in order to account for the adsorption observed the next morning, it is not clear whether the shift from A to B is a true measure of the change in optical response of the surface. This is because the parent film could still be annealing, and this effect decreases both α_m and $\Delta\alpha$. However, these effects are too slow to account for the observed decrease in $\delta(\Delta\alpha)$ at exposures greater than 1 torr. It is clear that these shifts signify

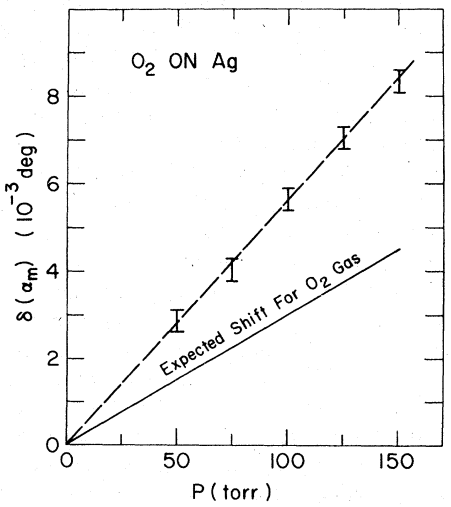

FIG. 8. Physical adsorption of O_2 on a Ag film after the chemisorption of oxygen has saturated. The solid line represents the shift expected for $\delta(\alpha_m)$ due to the presence of a uniform gas of O_2 next to the film.

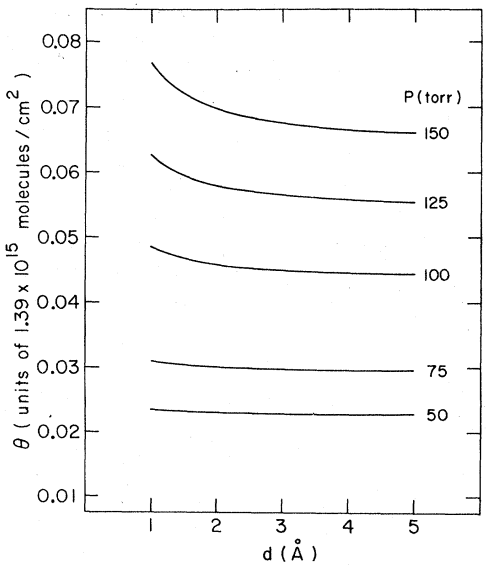

FIG. 9. Calculated coverage of physically adsorbed O_2 on Ag as a function of the thickness d_3 used in the solution of $D_4 = 0$.

a change in the chemical state of the adsorbate as manifested through its average optical response. This change in state could be shared by the adsorbate as a whole or could represent a change in the relative population of two adsorption states possessing different optical responses at 2 eV. It is possible that these shifts are associated with the formation of a second adsorption layer; however, the data of Kilty *et al.*[36] suggest that the coverage at 1 torr is of the order of half a monolayer of oxygen atoms for a (111) surface.

While exposing the film to 100 torr of O_2, we noticed that $\delta(\alpha_m)$ made a sudden jump increase upon exposure. Replacing the vacuum value of ϵ_4 by a value appropriate for a uniform gas of O_2 at 100 torr only accounted for part of the observed shift. Further, a shift of the same magnitude, but in the opposite direction, was observed when the gas was removed. Since no shifts in $\Delta\alpha$ were observed, we conclude that the shifts in $\delta(\alpha_m)$ indicate the presence of a physically adsorbed layer of O_2. These shifts are shown in Fig. 8 as a function of the equilibrium pressure. These data represent the average of several exposures on two films taken after extensive exposure at 100 torr to insure that the chemisorption was complete. The solid line represents the shifts expected by replacing the vacuum ϵ by a value appropriate for O_2 gas at the indicated pressure. We tried to extend this curve to higher pressures using data obtained by growing films without filling the glass liquid-nitrogen trap. This resulted in nonreproducible behavior for the chemisorption and often quenched the physisorption. Assuming that the atomic susceptibility of an O_2 molecule in the physisorbed state does not differ appreciably from its value in the gaseous state, the shifts in $\delta(\alpha_m)$ can be translated into values of coverage. Using a value for $4\pi\chi$ of 2.22×10^{-23} cm^3 and accounting for the chemisorption shifts by computing an effective ϵ_2 for the metal plus adsorbate, the computed values of $[\mathrm{Re}(\epsilon_3)-1]d_3/4\pi\chi$ determine the coverage. The value for the coverages obtained at the various exposure pressures plotted against the film thickness assumed to calculate them is shown in Fig. 9. The weak dependence of the coverage on d_3 implied by Eq. (24) is clearly evident. Because of the dilute coverages observed, it is not clear whether we are observing a density change of O_2 near the surface, the physical adsorption of O_2 on a chemisorbed layer of oxygen, or the occupancy of vacant Ag sites where the local configuration does not allow the formation of a chemical bond. However, unless the fractional number of vacant Ag sites is significantly larger than 7%, the observed linear dependence of coverage on pressure would argue against the latter interpretation.

The reaction of O_2 with Cu is stronger than the reaction of O_2 with Ag in that adsorption proceeds at measurable rates for exposure pressures less than 10^{-5} torr, and extensive exposure to O_2 results in the growth of an oxide layer. The relatively high sticking coefficient for O_2 on Cu allows us to estimate our coverages by assuming that all the O_2 admitted by expanding the gas in the bulb ultimately is adsorbed by the Cu. The response of the SPR to an exposure calculated to yield a coverage of 1×10^{15} atoms cm^{-2} is shown in Fig. 7. The points at lower coverage were obtained from the measured time dependence of $\delta(\alpha_m)$ and $\delta\alpha$. Upon exposure at higher pressures, the adsorption continues with the shifts tending to follow the dashed line until a new linear dependence is obtained at higher coverages. The solid line is the extrapolation of this linear region back to low coverages. The complete data are shown in Ref. 9. We interpret the low-coverage linear region as submonolayer and the high-coverage linear dependence as representing the growth of an oxide layer. The fact that an ordered structure of oxygen atoms on Cu(111) at 300 K has been observed,[42] corresponding to a coverage of 1.2×10^{15} atoms cm^{-2}, tends to confirm this interpretation.

It is interesting to examine the values of the effective dielectric function obtained from $D_4=0$ for the low-coverage linear region. In Fig. 10

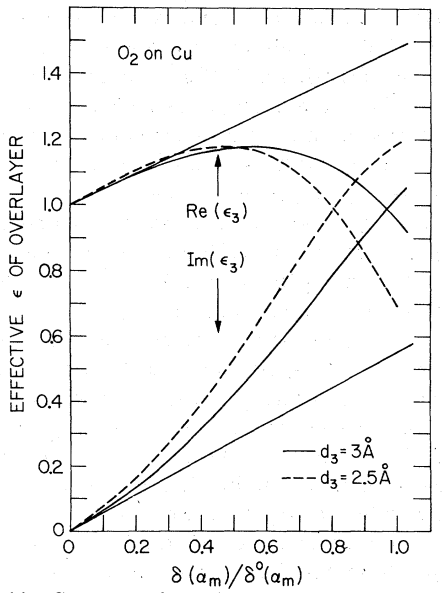

FIG. 10. Coverage dependence of the optical constant obtained by solving $D_4=0$ for the low-coverage Cu–oxygen data shown in Fig. 7. The abscissa is in units of the shift $\delta^\circ(\alpha_m)$ observed for the 1×10^{15}-atoms cm^{-2} exposure and is a monotonically increasing function of coverage. The straight lines are obtained by solving Eq. (24) in the limit of vanishing coverage.

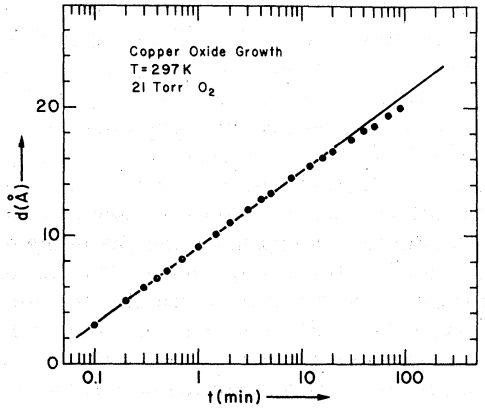

FIG. 11. Oxide thickness as a function of exposure time at 21 torr. The thicknesses were determined from $\delta(\alpha_m)$ using $\mathrm{Re}(\epsilon_{\mathrm{oxide}})=5.28$ in $D_4=0$.

we plot the values of ϵ_3 as a function of the ratio of $\delta(\alpha_m)$ used to compute ϵ_3 to $\delta^0(\alpha_m)$ corresponding to the 1×10^{15} exposure. This ratio is a monotonically increasing function of coverage. The solid curves are the real and imaginary parts of ϵ_3 computed for $d_3=3$ Å. The solid straight lines were computed by means of Eqs. (24) and (23) with $d_3=3$ Å. With the assumption that $\delta(\alpha_m)$ and $\delta(\Delta\alpha)$ are proportional to coverage, these lines correspond to a value of $(1.1+1.4i)\times10^{-24}$ cm^3 for the atomic susceptibility of an isolated oxygen atom in the adsorbed state. The strong dependence of ϵ_3 on the assumed value of d_3 used in $D_4=0$ is illustrated by the dashed curves which were computed for $d_3=2.5$ Å. The fact that $\mathrm{Re}(\epsilon_3)<1$ for $d_3=3$ Å at a concentration of 1×10^{15} implies that the adsorbate has an electronic resonance near 2 eV. The behavior of ϵ_3 as a function of coverage suggests that the width and position of this resonance are coverage dependent. The photoemission spectra of Tibbetts *et al.*[43] for oxygen adsorbed at room temperature on a Cu(100) surface indicate the presence of a transition near 1.4 eV associated with the Cu-O interface. This correspondence to our results may be fortuitous, as a similar analysis of our O_2 on Ag shifts also leads to a concentration-dependent resonance; however, these effects are less pronounced because $|\delta(\Delta\alpha)/\delta(\alpha_m)|$ is smaller. Also, the strength of the concentration dependence of the resonance can be lessened by assuming a larger value for d_3 for the overlayer.

The interpretation of the high-concentration linear dependence of $\delta(\Delta\alpha)$ on $\delta(\alpha_m)$ is less ambiguous because for an oxide layer one can assume ϵ_3 to be constant. The lossy Cu-oxide interface can be accounted for by defining an effective ϵ_2 determined by α_m of the Cu film and a $\Delta\alpha$ which is the sum of the clean Cu width and the width defined by the intercept of the extrapolated oxide response with the $\delta(\Delta\alpha)$ axis, Fig. 7. Assuming that $\mathrm{Re}(\epsilon_3)=5.28$, appropriate for a $CuO_{0.67}$ oxide layer,[44] the condition $D_4=0$ determines both d_3 and $\mathrm{Im}(\epsilon_3)$. A value of $\mathrm{Im}(\epsilon_3)=1.22$ was obtained for the thickness range 5–15 Å, which encompasses the observed region of linear dependence of $\delta(\Delta\alpha)$ on $\delta(\alpha_m)$. The determined dependence of $\delta(\alpha_m)$ on d_3 can be used to determine the rate of growth of the oxide layer. Figure 11 shows the oxide thickness versus exposure time for a second Cu film exposed and maintained at a pressure of 21 torr. A logarithmic dependence of thickness on exposure clearly is evident.

We now estimate the sensitivity limits of the SPR method to O_2 on Ag and Cu. No estimate for the chemisorbed state of oxygen on Ag can be made from our data although we have detected and measured 2% of a monolayer of physisorbed molecules on the surface. The sensitivity here is limited by the noise in the $\delta(\alpha_m)$ signal. We are more sensitive to the presence of O atoms adsorbed on Cu because of the large loss exhibited at 2 eV. Using our quoted sensitivity of 0.25% for $\Delta\alpha$ with a 0.1-sec time constant and assuming that the shifts $\delta(\Delta\alpha)$ in Fig. 6 are proportional to coverage, we estimate a detectability limit of about 0.6% of a monolayer of atoms where a monolayer is defined as one O atom for every Cu atom on a (111) surface.

C. 1,2-Dichloroethane

In order to demonstrate the systematic roughening of a surface, we decided to study the reaction of Ag with 1,2-dichloroethane vapor. Because the $Cl_2C_2H_4$ cannot be admitted through a liquid-nitrogen trap, we first exposed the Ag to O_2 at 100 torr in the hope that this passivated surface would be less responsive to residual gas contaminants when the cold trap was warmed. Thus the chemistry of the reaction is uncertain and we present the data at face value.

After extensive exposure to O_2, the liquid-nitrogen flask surrounding the glass trap was removed

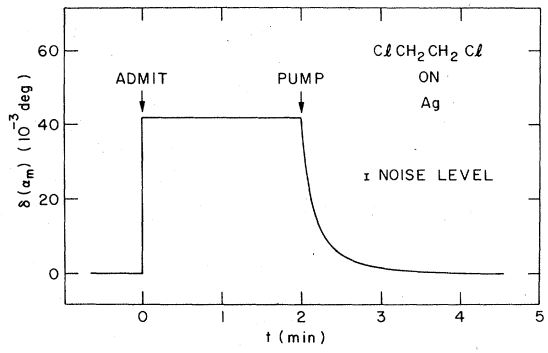

FIG. 12. Strong physical adsorption of 12.5 torr of 1,2-dichloroethane on a room-temperature Ag film previously exposed to 100 torr of O_2.

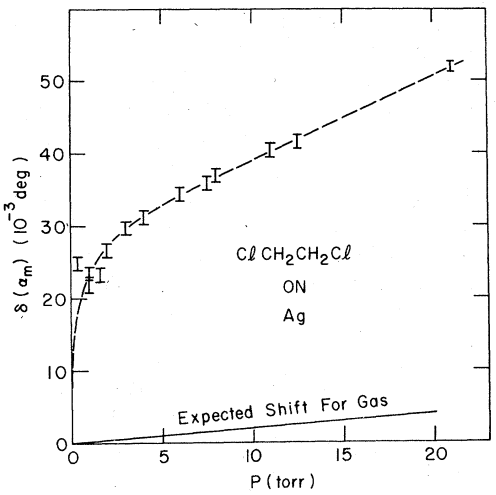

FIG. 13. Pressure dependence of the physical adsorption of 1,2-dichloroethane on room-temperature oxygen-exposed Ag. The ordinate is a monotonically increasing function of coverage.

and the SPR response was monitored. Just as the frost left the trap surface, α_m shifted but $\Delta\alpha$ did not. After two hours of pumping, the SPR was still shifted slightly from its value before the trap was warmed and $\Delta\alpha$ had narrowed a few percent, again indicating that some of the chemisorbed oxygen can be removed by pumping. When the film was exposed to a few torr of $Cl_2C_2H_4$, $\delta(\alpha_m)$ jumped rapidly and saturated, while no change in $\Delta\alpha$ was observed. Upon pumping, $\delta(\alpha_m)$ shifted back to a value smaller than before the exposure. This behavior continued for the next few exposures until no net shifts in $\delta(\alpha_m)$ were observed. Since the final SPR peak position is still shifted slightly from its value before the trap was warmed, we suspect that the dichloroethane only caused some of the contaminants adsorbed from the trap to desorb and did not remove any of the preadsorbed oxygen.

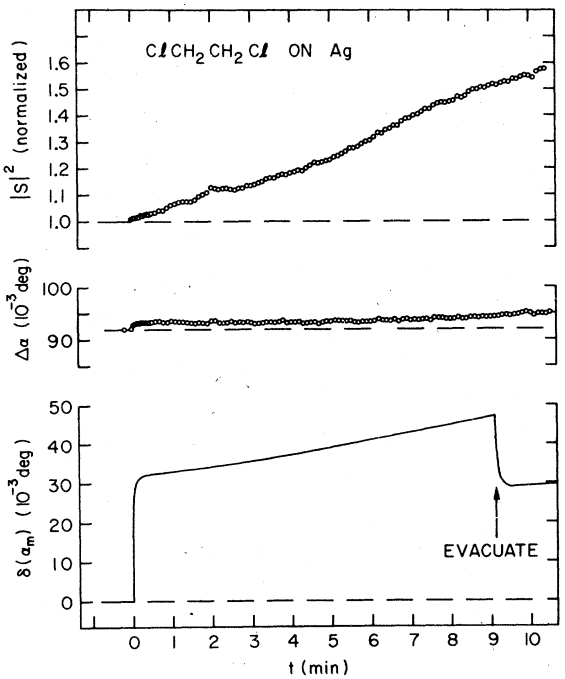

FIG. 14. Response of the SPR parameters on a 95°-C oxygen-exposed Ag film to ≈ 1 torr of 1,2-dichloroethane.

The results of a 12.5-torr exposure are shown in Fig. 12. The delayed response upon opening the pump valve indicates a measurable lifetime for the adsorption state of the molecule. By plotting the equilibrium $\delta(\alpha_m)$ against the exposure pressure, we obtain the adsorption curve shown in Fig. 13. The shift due to the background vapor (solid line) was calculated using the refractive index of 1.448 for the liquid and defining a molecular polarizability by partitioning the liquid susceptibility equally among the molecules. A crude estimate of coverage can be obtained by assuming a spherical molecule with a diameter of ≈ 6 Å as calculated from the liquid density. Then, an exposure pressure of ≈ 20 torr produces a shift which corresponds to a close-packed layer of dichloroethane "spheres". We therefore suspect that the marked curvature at a few torr may be associated with the completion of the first and the formation of the second adsorption layer. It is clear that a fair fraction of a monolayer is adsorbed at pressures less than 1 torr.

A strong physical adsorption is not the only reaction of dichloroethane with oxygen-passivated Ag surfaces at room temperature. After completing the adsorption measurements, we pumped on the film overnight. The next morning, we found the SPR significantly shifted and broadened, and that the scattered-light intensity had increased by at least an order of magnitude. These effects are presumably associated with trace amounts of dichloroethane left on the surface. These effects can be enhanced by reacting dichloroethane with a warm Ag surface. After growth at room temperature and exposure to O_2, we warmed the film by heating the entire sample chamber to ≈ 95°C. At this elevated temperature, little changes in the SPR was observed when the cold trap was removed. The film was now exposed to 1 torr of dichloroethane. The SPR response is shown in Fig. 14. Note the rapid uptake in correspondence with the physical adsorption observed at room temperature; however, $\delta(\alpha_m)$ does not saturate, instead it continues to increase. The $\Delta\alpha$ signal changes little, indicating either that the new adsorbate is not absorptive at low coverages or that a compensating change in state of the preadsorbed oxygen is occuring. The most dramatic effect is seen in the

$|S|^2$ signal, which steadily increases after exposure, indicating an increase in the surface roughness. After 9 min, we evacuated the chamber. Note that residual amounts of dichloroethane cause $|S|^2$ and $\delta(\alpha_m)$ to continue to increase. Subsequent exposures in the low-torr range further roughened the surface and broadened the resonance. After combined exposures totalling 3 torr-h, we obtained the values $\delta(\alpha_m)=0.185$ deg, $\delta(\Delta\alpha)=0.06$ deg, and $|S|^2\approx 65$. Although we have no knowledge of the detailed reactions taking place on the surface, it is clear that the surface topography is altered dramatically.

The measured increase in the surface-roughness scattering due to the reaction with dichloroethane can be used to establish an upper limit for the surface-roughness scattering contribution to the SPR width of the preexposed film. The quantity $[2\,\mathrm{Im}(k_{sp})]^{-1}$ is the attenuation length of a surface plasmon. Assuming that the intrinsic loss processes and the roughness-scattering losses are independent, we have

$$2\,\mathrm{Im}(k_{sp})=l_I^{-1}+l_R^{-1}\,, \tag{26}$$

where l_I and l_R are the attenuation lengths associated with the intrinsic and roughness losses of the metal [see Eq. (11)]. We now assume that the only effect of exposing to dichloroethane is to roughen the surface so that the increased width of the SPR represents radiation damping. Since $(1/l_R)$ is the energy radiated per unit distance traveled by the surface plasmon, we know that l_R decreases by a factor of ≈ 65 providing the intensity radiated along the film normal is proportional to the total radiated intensity. Solving simultaneously the equations valid before and after the exposure and using the measured values of k_{sp}, we obtain

$$l_R^{-1}/l_I^{-1}<0.01\,, \tag{27}$$

where l_R is the preexposed attenuation length. One can also compare the width after dichloroethane exposure to the width before O_2 exposure. This increases the right-hand side of the inequality by a factor of 1.5. Thus we conclude that the surface-roughness scattering contributions to our optical constants for the clean films are negligible.

ACKNOWLEDGMENTS

We would like to thank B. Poindexter for his assistance in constructing the apparatus and in making the measurements. We also thank S. L. McCarthy, L. C. Davis, and E. N. Sickafus for valuable discussions.

[1]A. Otto, Z. Phys. 216, 398 (1968).
[2]A. S. Barker, Jr., Phys. Rev. B 8, 5418 (1973).
[3]E. Kretschmann, Z. Phys. 241, 313 (1971).
[4]R. Bruns and H. Raether, Z. Phys. 237, 98 (1970).
[5]W. H. Weber and S. L. McCarthy, Phys. Rev. B 12, 5643 (1975).
[6]K. Holst and H. Raether, Opt. Commun. 2, 312 (1970).
[7]F. Abelès and T. Lopez-Rios, in *Proceedings of the First Taormina Research Conference on the Structure of Matter*, 1972, edited by E. Burstein and F. DeMartini (Pergamon, New York, 1974), p. 241.
[8]K. Bhasin, D. Bryan, R. W. Alexander, and R. J. Bell, J. Chem. Phys. 64, 5019 (1976).
[9]W. H. Weber, Phys. Rev. Lett. 39, 153 (1977).
[10]E. Kretschmann and H. Raether, Z. Naturforsch. Teil A 23, 2135 (1968).
[11]H. Raether, in *Physics of Thin Films*, edited by George Hass, Maurice H. Francombe, and Richard W. Hoffman (Academic, New York, 1977), Vol. 9, p. 145.
[12]E. N. Economou and K. L. Ngai, in *Advances in Chemical Physics XXVII*, edited by I. Prigogine and Stuart A. Rice (Wiley, New York, 1974), p. 265.
[13]A. W. Crook, J. Opt. Soc. Am. 38, 954 (1948).
[14]H. Wolter, in *Handbuch der Physik*, *Bd.* 24 (Springer, Berlin, 1956).
[15]E. Kretschmann, Opt. Commun. 5, 331 (1972).
[16]H. Kapitza, Opt. Commun. 16, 73 (1976).
[17]D. Hornauer, H. Kapitza, and H. Raether, J. Phys. D 7, L100 (1974).
[18]A. J. Braundmeier, Jr. and E. T. Arakawa, J. Phys. Chem. Solids 35, 517 (1974).
[19]D. L. Mills, Phys. Rev. B 12, 4036 (1975).
[20]E. Kretschmann, Opt. Commun. 10, 353 (1974).
[21]M. J. Dignam and M. Moskovits, J. Chem. Soc. Faraday Trans. 2 69, 65 (1973).
[22]H. E. Bennett, R. L. Peck, D. K. Burge, and J. M. Bennett, J. Appl. Phys. 40, 3351 (1969).
[23]H. Raether, in *The Structure and Chemistry of Solid Surfaces*, edited by G. A. Somorjai (Wiley, New York, 1969).
[24]R. C. O'Handley, D. K. Burge, S. N. Jasperson, and E. J. Ashley, Surf. Sci. 50, 407 (1975).
[25]G. A. Bootsma and F. Meyer, Surf. Sci. 14, 52 (1969).
[26]M. J. Dignam and M. Moskovits, J. Chem. Soc. Faraday Trans. 2 69, 56 (1973).
[27]T. Smith, J. Opt. Soc. Am. 58, 1069 (1968).
[28]R. W. Stobie, B. Rao, and M. J. Dignam, Surf. Sci. 56, 334 (1976).
[29]J. D. E. McIntyre and D. E. Aspnes, Surf. Sci. 24, 417 (1971).
[30]P. J. Feibelman, Phys. Rev. B 14, 769 (1976).
[31]W. H. Weber, S. L. McCarthy, and G. W. Ford, Appl. Opt. 13, 715 (1974).
[32]G. K. Boreskov and A. V. Khasin, Dokl. Akad. Nauk SSSR 177, 145 (1967) [Sov. Phys. Dokl. 177, 795 (1967)].
[33]M. M. P. Janssen, J. Moolhuysen, and W. M. H. Sachtler, Surf. Sci. 44, 553 (1974).
[34]P. G. Hall and D. A. King, Surf. Sci. 36, 810 (1973).
[35]A. W. Czanderna, J. Phys. Chem. 68, 2765 (1964).
[36]P. A. Kilty, N. C. Rol, and W. M. H. Sachtler, in *Proceedings of the Fifth International Congress on*

Catalysis, Miami, Florida. 1972, edited by J. Hightower (North-Holland, Amsterdam, 1973), p. 929.
[37]S. Evans, E. L. Evans, D. E. Parry, M. J. Tricker, M. J. Walters, and J. M. Thomas, Faraday Discuss. Chem. Soc. 58, 97 (1974).
[38]G. G. Tibbetts and J. M. Burkstrand, Phys. Rev. B 16, 1536 (1977).
[39]G. Rovida, F. Pratesi, M. Maglietta, and E. Ferroni, Surf. Sci. 43, 230 (1974).
[40]H. Albers, W. J. J. Van Der Wal, and G. A. Bootsma, Surf. Sci. 68, 47 (1977).
[41]W. M. H. Sachtler, Catal. Rev. 4, 27 (1970).
[42]G. W. Simmons, D. F. Mitchell, and K. R. Lawless, Surf. Sci. 8, 130 (1967).
[43]G. G. Tibbetts, J. M. Burkstrand, and J. C. Tracy, Phys. Rev. B 15, 3652 (1977).
[44]H. Wieder and A. W. Czanderna, J. Appl. Phys. 37, 184 (1966).